JOURNAL OF Materials CHEMISTRY

Sulfur K-edge X-ray absorption spectroscopy study of the reaction of zinc oxide with hydrogen sulfide

Clive E. Hayter,[a] John Evans,*[a] Judith M. Corker,[a] Richard J. Oldman[b] and B. Peter Williams[c]

[a]*University of Southampton, Highfield, Southampton, UK SO17 1BJ*
[b]*ICI Research & Technology Centre, P.O. Box 8, The Heath, Runcorn, UK WA7 4QD*
[c]*ICI Katalco, P.O. Box 1, Billingham, Cleveland, UK TS23 1LB*

Received 8th April 2002, Accepted 11th June 2002
First published as an Advance Article on the web 12th August 2002

We report *in situ* sulfur K-edge XAS data which show that a small number of very reactive sites are involved in the reaction of zinc oxide with hydrogen sulfide. Such sites react before the majority of the bulk oxide and are capable of forming zinc sulfide rapidly even at ambient temperatures. *In situ* sulfur K-edge EXAFS also provides evidence for a long sulfur–zinc interaction at 2.71 Å during the formation of bulk islands of zinc sulfide on the oxide. Powder diffraction and X-ray photoelectron spectroscopy on *ex situ* treated hydrogen sulfide absorbents confirm the formation of a twin phase material of crystalline zinc oxide and less crystalline zinc sulfide, both wurtzite polymorph, as suggested by EXAFS.

A significant problem for the petrochemical industry is the presence of sulfur containing feedstocks. Such compounds are not only unpleasant and toxic in nature, but also exhibit deleterious environmental and safety effects. In addition to this, many sulfur compounds act as catalyst poisons, for example the nickel alumina catalyst used in the steam reforming process is severely poisoned by sulfur donating electrons into the empty d orbitals of the metal thus blocking the active catalyst sites.[1] With the ever growing need to utilise oil and coal deposits containing high sulfur levels, methods of removing sulfur species have become well developed, however it is becoming increasingly important to understand the nature of the interaction between sulfur compounds and heterogeneous catalysts.

The focus of the present experiments is in the process train from natural gas (or similar feedstock) to hydrogen manufacture by steam reforming. Due to the variety of sulfur compounds encountered, most manufacturers now use a two stage process for sulfur removal. The first involves reaction of the crude feedstock with hydrogen over a nickel or cobalt molybate catalyst (hydrodesulfurization, HDS) to produce hydrocarbons and hydrogen sulfide. The second stage of sulfur removal, is reaction of the hydrogen sulfide produced by the HDS catalyst (or present in the feedstock anyway) with a bed of porous zinc oxide according to eqn. (1). Reaction of hydrogen sulfide with zinc oxide is favoured under almost all process conditions and it is possible to reduce the level of gas exiting the bed to less than 0.02 ppm.

$$ZnO + H_2S \rightarrow ZnS + H_2O \quad (1)$$

A substantial amount of work has been carried out on sulfur adsorption by metal oxides. Westmoreland and Harrison[2] first identified the potential for desulfurization of a number of oxides (Fe, Zn, Mo, Mn, V, Ca, Sr, Ba, Co, Cu, and W) at high temperatures (>300 °C). A further study by the same authors[3] compared the kinetics of the reaction of hydrogen sulfide with four of these oxides (MnO, CuO, ZnO, V_2O_3) using a thermobalance technique to measure global reaction rates. Results indicated the potential of several systems including manganese oxide (MnO) and zinc oxide (ZnO) and that the reactions were all first order with respect to hydrogen sulfide. Jalan[4] and Yumura[5] both studied desulfurization potential at high temperatures and in the latter of these two reports zinc oxide was shown to have the largest capacity for desulfurizing gases at high temperatures when capacity was expressed per unit of surface area.

Under normal conditions the equilibrium of eqn. (1) is strongly in favour of sulfide formation, but the overall rate is controlled by both pore diffusion and lattice diffusion.[6] As a result of these effects, all of the oxide may not be converted to sulfide in a sensible time. The dependence of the process on lattice diffusion can be reduced by making a zinc oxide with a large internal surface area. Unfortunately such a material would have a low mechanical strength, making it difficult to handle. Strength and density could be increased by compaction, but this material would then have a low porosity. This problem has been overcome commercially by using zinc oxide plus a cement support such as calcium oxide or alumina.[1] Carnell and Denny[7] investigated the operation of such an absorbent under typical process conditions using energy dispersive X-ray microanalysis (EDX) and their work showed that sulfur was absorbed from the outside of each granule of absorbent and that where the absorbents were too dense an impervious layer of zinc sulfide is formed around the granules making utilisation of the inner core difficult.

Significantly very little structural evidence exists on the mechanism of the reaction between hydrogen sulfide and the oxide based absorbents, as empirical operation has taken precedence. Structural elucidation of the mechanism of reaction would considerably aid the design of future absorbents with enhanced operating characteristics. As a consequence of this we report here further observations of the reaction using the technique of *in situ* sulfur K-edge XAS. The work follows on from a preliminary study by ourselves[8] on the same absorbents in which we first outlined the use of the *in situ* soft XAS technique and proposed a mechanism involving the formation of islands of zinc sulfide on the oxide surface, which as the reaction proceeds, eventually form bulk regions of zinc sulfide.

 DOI: 10.1039/b203426n

Experimental

Powder X-ray diffraction (XRD)

Phase identification of the absorbents was performed using powder diffraction. Patterns were recorded on a Siemens D5000 diffractometer operating at 40 kV, 35 mA. Cu-K_α radiation was provided by an X-ray tube fitted with a primary monochromator. Samples were mounted after fine grinding in recessed aluminium holders and data were collected in the 2θ range 20–80°. Data analysis was performed using the Siemens Diffrac 500 software package, which allowed access to the JCPDS Powder Diffraction files enabling comparison with the experimental data and assessment of the phases present.

X-Ray photoelectron spectroscopy (XPS)

XPS data were all recorded on a VG ESCALAB 200D XPS spectrometer using a monochromatorized rotating Mg anode source with incident K_α radiation of 1253.6 eV. All samples were prepared by finely grinding them and then sprinkling loosely on stainless steel stubs covered in double sided conducting tape. Charge correction was performed by referencing to the carbon 1s line at 285.6 eV, present as the hydrocarbon content in all samples. Data analysis was performed on a VAX computer interfaced to the instrument. Quantification was obtained on constituent elements in each sample using database sensitivity factors. Comparison of chemical shift values was made either with data obtained experimentally on standard materials or from the literature.

X-Ray absorption spectroscopy (XAS)

The X-ray absorption spectroscopy (XAS) experiments detailed here, were all carried out using Station 3.4 of the Synchrotron Radiation Source (SRS), Daresbury Laboratory. The synchrotron operated in multibunch mode with an electron beam energy of 2 GeV and a beam current varying from 160 to 220 mA. Sulfur K-edge (2472 eV) data were recorded using a InSb(111) double crystal monochromator. Harmonic rejection was provided by a grazing incidence pre-mirror which acted as a high energy filter. Reference measurement (I_o) was achieved through the use of a foil through which the beam passed and the current measured and amplified using a Keithley current amplifier. Data were almost exclusively recorded in fluorescence mode using a gas proportional counter operating at 4 kV and containing a 50 : 50 v/v helium–argon mixture. Count rates were maximised to 200 kHz at the peak of the white line. Standard samples were prepared by diluting the sample in dry boron nitride (5% by weight of sulfur) and then dropping as an acetone slurry on to an aluminium holder. Alternatively samples were diluted in boron nitride and pressed into 16 mm diameter disks and mounted on the *in situ* cell using vacuum grease. Pure oxide samples used for the *in situ* experiments were also prepared in this manner. All samples were calibrated with respect to the K-edge of elemental sulfur at 2472 eV.

Data analysis (EXAFS)

Background subtraction to extract the EXAFS oscillations from the experimental absorption was carried out in this work using the PC based program PAXAS.[9] Curve fitting of a model to the extrapolated EXAFS was achieved using the program EXCURV92.[10] Phaseshifts are calculated within the program using *ab initio* methods and a least squares refinement was performed on the EXAFS derived structural parameters to minimise the overall *R*-factor. A second measure of the overall goodness of fit is the fit index (FI) that measures the sum of the square of the differences between the theoretical and experimental data points. Statistical tests were also used to assess the significance of each shell and whether too many parameters had been included in a particular refinement. Joyner *et al.*[11] suggested that if a reduction in the fit index is satisfied by $FI_{n+1}/FI_n < 0.96$ then the new shell is significant. In this work only shells that are significant at the 99% probability level in accord with this test are included.

Finally the number of adjustable parameters did not exceed the number of independent data points ($N_{idp} = 2\Delta k \times \Delta r/\pi$), where Δk is the difference in k space and Δr the difference in r space between the closest and most distant shells being fitted.

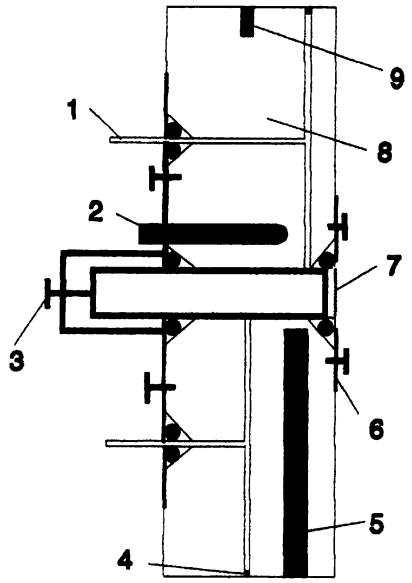

Fig. 1 Cross sectional diagram of the cell for the *in situ* chemistry whilst studying the sulfur K-edge X-ray absorption spectra (1. 1/8″ stainless steel tubing, 2. K-type thermocouple, 3. adjustment screw, 4. stainless steel plug, 5. cartridge heater, 6. clamping plate, 7. 13 μm Kapton window, 8. stainless steel block, 9. threaded connection).

Experimental equipment

In situ monitoring of chemistry at the sulfur K-edge was performed using the cell shown in Fig. 1. The cell is a compact design based around a stainless steel cylinder. Through the middle of the cell runs a circular piston or plunger that moved horizontally on an adjustment screw. Vacuum tight seals were made at the front and back of this plunger but gas was able to circulate internally through the cell *via* drilled gas lines. A 200 W, 240 V cartridge heater and a K-type thermocouple were inserted into the base of the cell. Finally a coil of 1/8″ stainless steel tubing was welded to the exterior of the cell to allow cyclic delivery of coolant.

Loading was performed by cementing a pressed disk sample onto the front end of the plunger using vacuum grease and covering with a 13 μm Kapton[12] window. The cell was then connected up to the gas manifold depicted in Fig. 2. The manifold consisted of a pressure gauge, valves, a hydrogen sulfide lecture bottle, a liquid nitrogen trap for removal of excess gas and connection to a vacuum supply. Electrical leadthroughs into the He-chamber also allowed connection of the thermocouple probe and the temperature controller. In addition to the basic apparatus the low temperature experiments (see below) required the use of a cryostat system developed by Andrews *et al.*[13] This gave a full experimental temperature range of −40 to 180 °C.

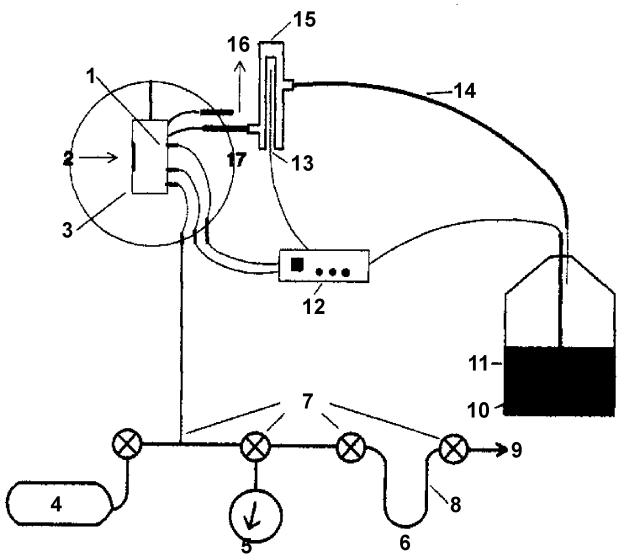

Fig. 2 Experimental layout for *in situ* sulfur X-ray absorption spectroscopy (1. heater, 2. incident X-rays, 3. cell, 4. H_2S lecture bottle, 5. gauge, 6. trap, 7. valves, 8. gas manifold, 9. vacuum pump, 10. heater, 11. dewar, 12. temperature controller, 13. line heater, 14. flexible dewar, 15. transfer dewar, 16. N_2 vent, 17. beamline chamber).

Results and discussion

Ex situ treated absorbents and standard sulfur containing compounds

Since the normal plant lifetime of the commercially available absorbents is between 2 and 5 years, a model experiment was developed to mimic the plant desulfurisation of natural gas or napthala. Fig. 3 shows the experiment performed. The experimental set up consisted of tightly packed beds of a commercially available absorbent[1] through which a 5% hydrogen sulfide/nitrogen or hydrogen sulfide/methane mixture was passed for several hours until H_2S was detected at the base of the column along with water. Numbers were assigned to the absorbent according to its position in the reactor as shown in Fig. 3. In this case the column was operated at 370 °C to mimic plant desulfurisation.

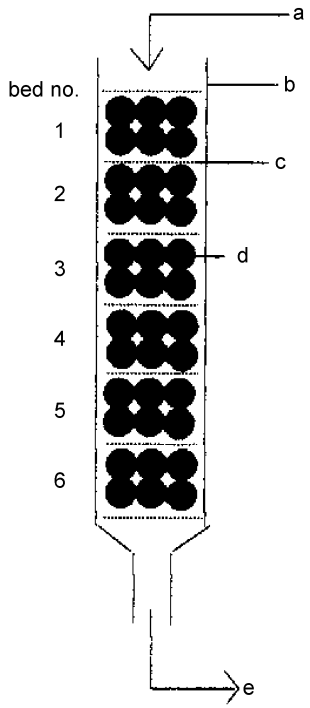

Fig. 3 *Ex situ* reaction of zinc oxide absorbent (a. 5% H_2S/CH_4 or 5% H_2S/N_2, b. glass column, c. metal gauze, d. absorbent granule, e. H_2O).

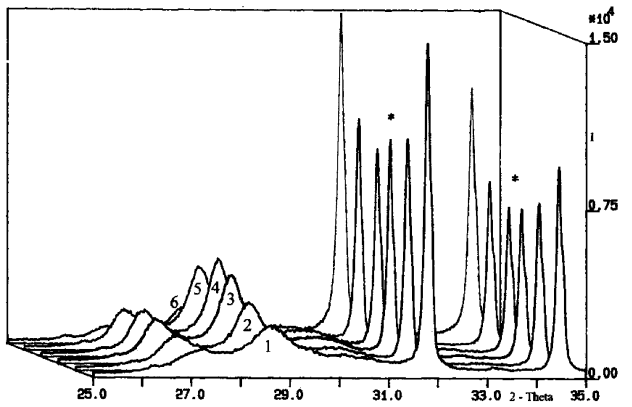

Fig. 4 Powder X-ray diffraction patterns of *ex situ* treated zinc oxide absorbent (* peaks due to ZnO, beds 1–6 marked).

Diffraction profiles for these *ex situ* treated absorbents showed them to contain very little non-crystalline material. The diffraction patterns for the sample beds are depicted in Fig. 4 and qualitative analysis using the JCPDS files revealed a major phase of highly crystalline zinc oxide (wurtzite), a minor less crystalline phase of zinc sulfide (wurtzite) and a trace of calcium carbonate (aragonite). The level of detectable sulfur also varied between the beds of absorbent, increasing up to bed 4, bed 5 containing slightly less and bed 6 containing the least. A similar experiment using pure zinc oxide (Aldrich 99.998%) was also carried out under identical conditions and despite the fact that considerably less sulfur was present in the samples, a zinc oxide and zinc sulfide phase were identified.

XPS data for the *ex situ* treated absorbents is detailed in Table 1. Highlighted also within Table 1 are relevant data for standard sulfur containing materials together with calculated peak area.

Revealed in Table 1 is evidence for a double component oxygen 1s line in the spectra for pure zinc oxide and for the absorbent beds. This species leads to clear asymmetry in the oxygen line for these materials and can be easily separated out from the oxide component. In separating out these oxygen components individual values are quoted for each oxygen component and the surface zinc to oxide ratio in the sample of zinc oxide is 1 : 1 as expected. The relative proportions of

Table 1 XPS derived parameters for standard materials and *ex situ* treated oxide absorbents (*peak area ratios shown in italics*)

Compound	Binding energy/eV (*atom ratio*)			
	Zn 2p	O1 1s	O2 1s	S 2p
ZnO	1021.6	530.2	531.9	
	(1.00)	*(1.01)*	*(0.56)*	
ZnS	1022.6	-	532.3	161.9
	(1.00)		*(0.57)*	*(1.48)*
$ZnSO_4 \cdot 7H_2O$	1023.6	-	532.4	170.1 , 160.9
	(-)		*(-)*	*(-), (-)*
ZnO 32-4 bed 1	1021.9	530.5	531.8	161.8
	(1.00)	*(0.38)*	*(0.74)*	*(1.38)*
ZnO 32-4 bed 2	1022.1	531.1	532.1	161.9
	(1.00)	*(0.09)*	*(0.39)*	*(1.21)*
ZnO 32-4 bed 3	1022.0	530.5	532.1	161.9
	(1.00)	*(0.04)*	*(0.83)*	*(1.36)*
ZnO 32-4 bed 4	1022.0	530.7	532.0	161.8
	(1.00)	*(0.02)*	*(0.98)*	*(1.53)*
ZnO 32-4 bed 5	1021.6	530.4	531.8	161.9
	(1.00)	*(0.48)*	*(0.27)*	*(1.15)*
ZnO 32-4 bed 6	1021.6	530.3	532.2	162.0
	(1.00)	*(1.01)*	*(0.21)*	*(0.27)*

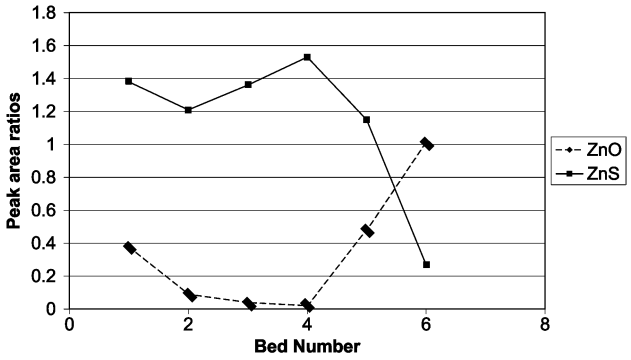

Fig. 5 Graph of XPS derived quantification ratios for the series of absorbent materials.

surface zinc to sulfur and zinc to oxygen are depicted graphically for the absorbent beds in Fig. 5. This graph shows that the Zn : S ratio correlates well with that found by powder diffraction *i.e.* an increase in sulfur to bed 4 then beds 5 and 6 show a decrease. The oxide component mirrors the profile trend in detectable sulfur showing a maximum in bed 6.

One final point apparent from the data for the absorbent beds is that a small but distinct chemical shift is evident in the zinc $2p_{3/2}$ photoelectron line, this is most prevalent between bed 4 (containing the most sulfide) and bed 6 (containing the least). Further these shifts correlate well to those in found in zinc oxide and zinc sulfide.

Fig. 6 shows sulfur K-edge XANES spectra for the standard materials (phase purity assessed by XRD where appropriate), native sulfur and hydrogen sulfide gas. Fig. 7 highlights the shift in energy when traversing the series sulfide to sulfite and sulfate. Indeed a shift of *ca.* 8–10 eV is recorded on moving from sulfide to sulfate. Evident also in these spectra are very strong white lines for the sulfur–oxygen systems, which serve

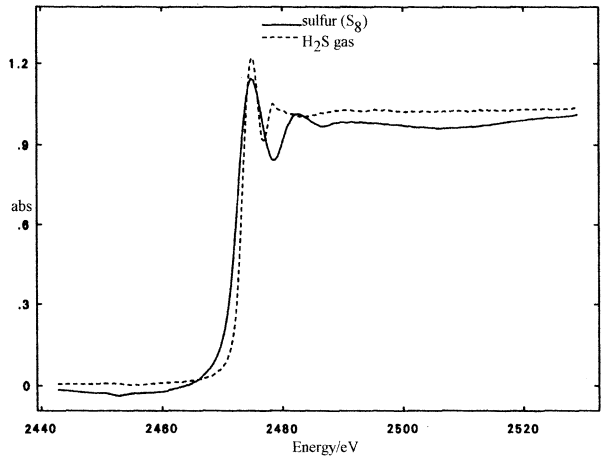

Fig. 6 Sulfur K-edge XANES spectra for sulfur (S_8) and H_2S.

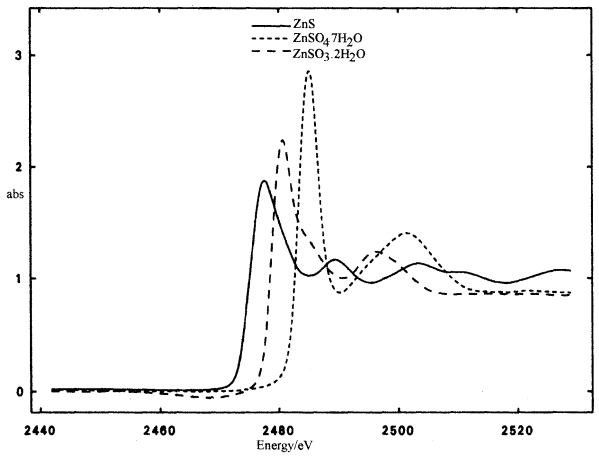

Fig. 7 Sulfur K-edge XANES spectra for ZnS, $ZnSO{\cdot}2H_2O$ and $ZnSO_4{\cdot}7H_2O$.

to illustrate the richness of features in this region and its usefulness in qualitative analysis of different sulfur systems.[14,15] Table 2 shows full sulfur K-edge EXAFS derived parameters for these standard materials. Interatomic distances obtained by curve fitting of the EXAFS are also compared with those quoted in the literature obtained from single crystal X-ray diffraction. The agreement between experiment and theory is lower than generally observed for higher energy edges with longer reliable data lengths.

Sulfur K-edge EXAFS data for the *ex situ* treated absorbent materials has been reported previously in a preliminary investigation by ourselves.[8] The results obtained were consistent with the formation of a zinc sulfide phase on the oxide absorbent. Significantly in the absorbents studied the coordination numbers of the non-bonded shells were reduced compared to zinc sulfide (Table 2), suggesting only a short range order existing in the absorbent materials.

In situ treated zinc oxide absorbents

Commercially available absorbent, dehydrated zinc oxide (350 °C, 6 hours, 10^{-6} Torr; Aldrich 99.998%) and pure zinc oxide (Aldrich 99.998%) were all treated with hydrogen sulfide (Aldrich 99.8%) *in situ* using a variety of experimental protocols. No significant reactivity or structural differences were identified in using a commercial absorbent, therefore, we report here the results for zinc oxide as these are definitive.

A preliminary *in situ* experiment was reported previously[8] using dehydrated zinc oxide and the results of this static treatment type experiment at 50 °C indicated a smooth progression of states from chemisorbed H_2S or HS^- to a zinc sulfide type phase consistent with those of the *ex situ* treated samples. No significant change in oxidation state of the sulfur species was identified from qualitative analysis of the sulfur K-edge XANES spectra. Powder X-ray diffraction of

Table 2 Sulfur K-edge EXAFS derived structural parameters[16,17] for standard sulfur containing materials (e.s.d.s in parentheses)

Compound	*R* factor (%)	Coordination number	*R*/Å	$2\sigma^2$/Å	Diffraction data/ Å
Sulfur (S_8)	46	1 S	1.938(4)	0.014(1)	(2 S) 2.04[18]
		1 S	3.249(5)	0.003(2)	(2 S) 3.31
$ZnSO_4.7H_2O$	39	4 O	1.422(2)	0.005(1)	(4 O) 1.46[19]
$ZnSO_3.2H_2O$	45	3 O	1.469(5)	0.011(1)	(3 O) 1.55[20]
		3 Zn	3.311(5)	0.020(3)	(3 Zn) 3.16
ZnS	27	4 Zn	2.296(1)	0.009(1)	(4 Zn) 2.34[21]
(wurtzite)		12 S	3.752(6)	0.023(1)	(12 S) 3.82
		12 Zn	4.420(4)	0.018(1)	(12 Zn) 4.48

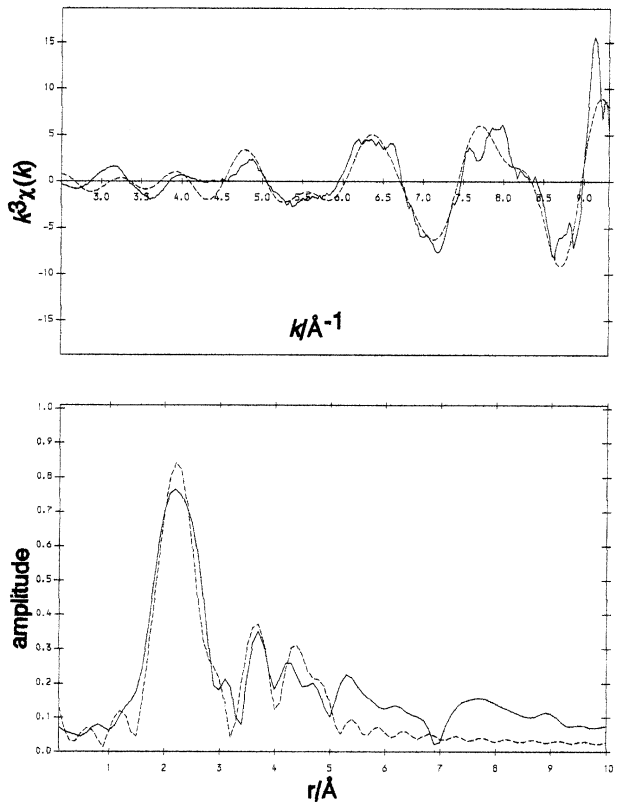

Fig. 8 *In situ* sulfur K-edge EXAFS and Fourier transform (phaseshift corrected for Zn) of the reaction of H_2S with ZnO (experimental, spherical wave theory).

this sample (not reported) revealed that the material was composed of at least 10% crystalline zinc sulfide (wurzite).

Fig. 8 shows the sulfur K-edge EXAFS of a similarly dehydrated sample of zinc oxide (1.5 g; 0. 18 mol) which was treated with hydrogen sulfide (0.75 atm) this time at room temperature (23 °C). Unlike the previous experiment and, rather surprisingly, the presence of EXAFS occurred very quickly on the reaction timescale and suggests a speedy transition to a stable zinc sulfide type phase. EXAFS derived structural parameters (Table 3) confirm the presence of a zinc sulfide type phase. Powder diffraction analysis of the sample revealed that the system contained less than 1% crystalline zinc sulfide (wurtzite).

The results presented in Fig. 8 raise ambiguities concerning the *in situ* data reported previously. For instance the process appears to show a smooth progression of states at 50 °C and yet at room temperature a speedy transition to a zinc sulfide like final state is evident. These data can be explained, in considering that using a static pulse type experiment, we could in theory be characterising effects due to hydrogen sulfide in the gas phase as well as changes in the solid state. Qualitative analysis of the absorbance spectrum for the latter data set does in fact reveal that the oscillations due to zinc sulfide are in fact very weak and that the majority of the edge intensity is probably due to hydrogen sulfide gas. In the previously reported data, oscillations due to zinc sulfide were much more intense, indicating a more extensive bulk phase of sulfide. These conclusions are confirmed by the powder diffraction data.

In summary the data obtained on the system so far suggests that a proportion of the oxide reacts very quickly producing zinc sulfide even at low temperatures, the majority of the material however reacting much more slowly to form the bulk phase.

To eliminate the problem of composite effects between the gas phase and solid state species in the static pulse protocol, a dynamic pulse protocol was developed. In this experiment the hydrogen sulfide is removed after an exposure time and before the sample was characterised *in situ*. The sulfur K-edge EXAFS data of the reaction between zinc oxide (0.8 g, 8 mmol.) and hydrogen sulfide following a pulse of 1 atm of gas for 3 minutes at 35 °C are presented in Table 3. The EXAFS spectra reveal a fingerprint pattern very similar to zinc sulfide and confirm the presence of reactive sites in the oxide. The distances obtained show reasonable agreement with the standard zinc sulfide sample (Table 2) except for the shell containing four zinc atoms at a distance of 2.71 Å. This interaction significantly improves the overall fit of the model and yet the interatomic distance obtained shows no correlation with any known distances in the zinc–sulfur compounds analysed (Table 2).

In an attempt to characterise earlier stages of the process occurring at these active sites, three subsequent experiments were carried out, each progressively reducing the exposure time of the oxide from 2 minutes to 30 seconds. In all cases only a zinc sulfide type spectrum was obtained. Further experiments were then performed in which the concentration of hydrogen sulfide was reduced through dilution with nitrogen, for example a typical experiment comprised of adding 1 atm of a 0.5 H_2S/0.5 N_2 mixture for 1 minute at 11 °C. This also, unfortunately, yielded spectra similar to that of zinc sulfide.

Clearly the process was proceeding too quickly at the active sites for characterisation on the timescale of the experiment at ambient temperatures. Fig. 9 depicts a stack plot of sulfur K-edge XANES spectra recorded following the addition of a pulse of 1.2 atm H_2S for 40 minutes to ZnO (0.5 g, 6.1 mmol.) at an initial temperature of −24 °C which was subsequently raised to 24 °C during the reaction. A 40 minute pulse was used in this particular experiment as this was identified as giving a useful signal to noise ratio. It is clear from this stack plot that the reaction at the active sites follows a pathway identical to that in the bulk, previously reported. Table 3 shows the results

Table 3 *In situ* sulfur K-edge EXAFS derived structural parameters[16,17] for the reaction between H_2S and ZnO (e.s.d.s in parentheses)

Treatment	Coordination number	R/Å	$2\sigma^2$/Å	R factor (%)
ZnO + H_2S	2.2(1) Zn	2.314(2)	0.0072(6)	45
	4.1 (2) S	3.879(6)	0.0090(2)	
	4.4 (4) Zn	4.425(1)	0.0087(1)	
Pulsed reaction of ZnO + H_2S	4.1(1) Zn	2.273(2)	0.0162(2)	69
	5.4(6) S	3.67(2)	0.013(4)	
	4.8(4) Zn	3.712(6)	0.01222(2)	
Pulsed reaction of ZnO + H_2S at −24 °C	4.6(8) Zn	2.28(1)	0.041(2)	63

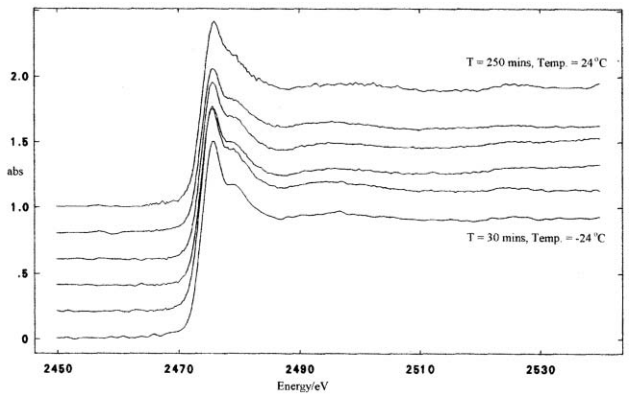

Fig. 9 *In situ* sulfur K-edge XANES of the reaction of H_2S with ZnO after a pulsed experiment at −24 °C. Spectra recorded at 44 minute intervals.

of analysis of *in situ* sulfur K-edge EXAFS recorded at $t = 383$ minutes after the addition of hydrogen sulfide to the system. Although the data is of poor quality, it is evident that a sulfur–zinc interaction may be modelled to the data at a distance similar to that found in zinc sulfide (blende).

Conclusion

These studies have shown that the sulfur K-edge XANES region is rich in information and is a useful tool in phase identification of sulfur in its various forms both in standard materials and unknowns. Refinement of sulfur K-edge EXAFS data obtained on standard sulfur containing materials has also afforded valuable information. The experiments we have described also show that the recording of *in situ* data at the sulfur edge is possible and open up the possibility of future studies with significant potential in investigating for example catalytic poisoning by sulfur under real industrial operating conditions.

The XPS and XRD data presented in this investigation for the *ex situ* treated absorbents in their final states has confirmed the theory suggested previously[8] of a twin phase material consisting of crystalline zinc oxide (wurtzite) and a less ordered phase of zinc sulfide (wurtzite). It is important to point out that in this case the sulfide phase does not adopt the thermodynamically more stable blende structure, instead adopting the wurtzite polymorph and thus avoiding extensive structural reorganisation of the material.

EXAFS analysis of *in situ* treated zinc oxide yields results consistent with those found for the *ex situ* treated samples and in all cases a reduction in coordination numbers and hence long range order is evident in the materials. Both pulsed and static experiments lead to similar conclusions of a small number of very active sites on the surface of the oxide which react extremely quickly even at ambient temperatures to form zinc sulfide. These sites then act as nucleating centres for the growth of the sulfide phase throughout the remainder of the oxide.

The results presented here and in a preliminary study[8] are consistent with a mechanism of formation involving dissociative chemisorption of hydrogen sulfide, most probably at an anion vacancy site. This leads to the formation of surface islands of zinc sulfide which almost certainly involve distortion of the regular wurtzite structure and lead to the formation of long sulfur to zinc bonds. These islands then develop by migration of sulfide ions through the oxide lattice eventually forming bulk regions of zinc sulfide.

Acknowledgements

The authors wish to thank ICI Chemicals & Polymers and the University of Southampton for funding this work. We also wish to thank CLRC for access to the SRS at Daresbury Laboratory. We dedicate this paper to the memory of Judith Corker.

References

1 P. J. H. Carnell, *Catalyst Handbook*, ed. M. V. Twigg, Wolfe Publishing Ltd., London, 2nd edn., 1989, ch. 4, p. 191, pp. 215–217.
2 P. R. Westmoreland and D. P. Harrison, *Enivron. Sci. Technol.*, 1976, **10**, 659.
3 P. R. Westmoreland, J. B. Gibson and D. P. Harrison, *Enivron. Sci. Technol.*, 1977, **11**, 488.
4 V. Jalan, *Proc. Int. Gas Res. Conf.*, 1981, 291.
5 M. Yumura and E. Furminsky, *Ind. Eng. Chem. Proc. Des. Dev.*, 1985, **24**, 1165.
6 Y. V. Furmer, V. I. Kosorotov, O. I. Brui, R. N. Proning and V. I. Kolomin, *Sov. Chem. Ind. (Engl. Transl.)*, 1978, **11**, 158.
7 P. J. H. Carnell and P. J. Denny, in *Ammonia Plant Safety and Related Facilities*, American Institute of Chemical Engineers, New York, 1985.
8 J. Evans, J. M. Corker, C. E. Hayter, R. J. Oldman and B. P. Williams, *Chem. Commun.*, 1996, 1431.
9 N. Binsted, PAXAS, Program for the analysis of X-ray absorption spectra, University of Southampton, 1988.
10 N. Binsted, J. M. Campbell, S. J. Gurman and P. C. Stephenson, EXCURV92, CLRC Daresbury Laboratory, 1992.
11 R. W. Joyner, K. J. Martin and P. Meehan, *J. Phys. C*, 1987, **20**, 4005.
12 Kapton,™ Polyimide, Goodfellow Ltd., Cambridge Science Park, UK.
13 P. Andrews, PhD Thesis, University of Southampton, 1993.
14 C. L. Spiro, J. Wong, F. W . Lytle, R. B. Greegor, D. H. Maylotte and S. H. Lamson, *Science*, 1984, **226**, 48.
15 G. N. George and M. L. Gorbatty, *J. Am. Chem. Soc.*, 1989, **113**, 3182.
16 J. M. Corker, J. Evans, H. Leach and W. Levason, *J. Chem. Soc., Chem. Commun.*, 1989, 181.
17 B. K. Teo, *EXAXS, Basic Principles and Data Analysis*, Springler-Verlag, Berlin, 1986; S. J. Gurman, in *Application of Synchrotron Radiation*, ed. C. R. A. Catlow and G. N. Greaves, Blackie, Glasgow, 1989.
18 S. J. Rettig and J. Trotter, *Acta Crystallogr., Sect. C*, 1987, **43**, 2260.
19 M. Calleri, A. Gavetti, G. Ivaldi and M. Rubbo, *Acta Crystallogr., Sect. B*, 1984, **40**, 218.
20 H. Quinones and S. Baggio, *J. Inorg. Nucl. Chem.*, 1972, **34**, 2153; B. Nyberg, *Acta Chem. Scand.*, 1972, **27**, 1541.
21 E. H. Kisi and M. M. Elcombe, *Acta Crystallogr., Sect. C*, 1989, **45**, 1867; E. A. Jumpertz, *Z. Elektrochem.*, 1955, **59**, 419.